

TextInPlace: Indoor Visual Place Recognition in Repetitive Structures with Scene Text Spotting and Verification

Huaqi Tao¹, Bingxi Liu^{1,2}, Calvin Chen³, Tingjun Huang¹, He Li¹, Jinqiang Cui², and Hong Zhang^{1,*}, *Life Fellow, IEEE*

Abstract—Visual Place Recognition (VPR) is a crucial capability for long-term autonomous robots, enabling them to identify previously visited locations using visual information. However, existing methods remain limited in indoor settings due to the highly repetitive structures inherent in such environments. We observe that scene texts frequently appear in indoor spaces and can help distinguish visually similar but different places. This inspires us to propose TextInPlace, a simple yet effective VPR framework that integrates Scene Text Spotting (STS) to mitigate visual perceptual ambiguity in repetitive indoor environments. Specifically, TextInPlace adopts a dual-branch architecture within a local parameter sharing network. The VPR branch employs attention-based aggregation to extract global descriptors for coarse-grained retrieval, while the STS branch utilizes a bridging text spotter to detect and recognize scene texts. Finally, the discriminative texts are filtered to compute text similarity and re-rank the top-K retrieved images. To bridge the gap between current text-based repetitive indoor scene datasets and the typical scenarios encountered in robot navigation, we establish an indoor VPR benchmark dataset, called Maze-with-Text. Extensive experiments on both custom and public datasets demonstrate that TextInPlace achieves superior performance over existing methods that rely solely on appearance information. The dataset, code, and trained models are publicly available at <https://github.com/HQiTao/TextInPlace>.

I. INTRODUCTION

Visual Place Recognition (VPR) is a global localization task based on image retrieval, which aims to find images from a reference image database that represent the same place as the query image [1]. It is widely applied in autonomous vehicles, augmented reality devices, and service robots. The paradigm of VPR typically involves training neural networks on large-scale datasets to encode images into compact global descriptors and retrieving the most similar images based on the similarity of these descriptors [2]. During the past decade, researchers have conducted extensive studies to address challenges such as database scale [3], viewpoint variations [4], illumination changes [5], seasonal transitions [6] and computational efficiency [7], leading to remarkable advancements.

However, state-of-the-art (SOTA) VPR methods often struggle in indoor scenarios, suggesting that indoor VPR

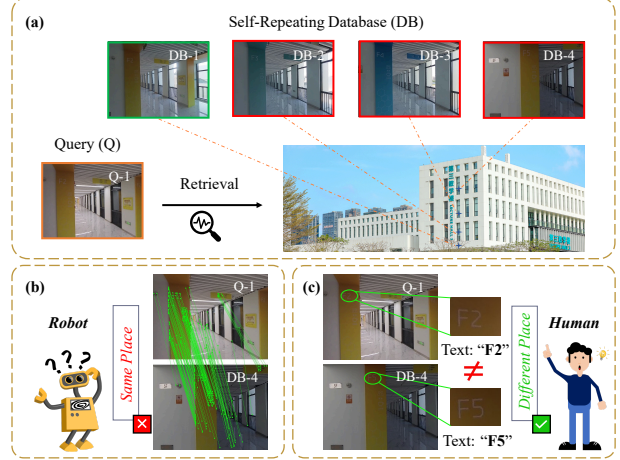


Fig. 1. (a) In multi-floor buildings, there are many locations that appear highly similar but are actually different. (b) When robots rely solely on appearance information, they may mistakenly identify images of these locations as the same place. (c) In contrast, humans can utilize textual clues in the environment to accurately distinguish these highly similar places.

remains an underexplored research area. Moreover, indoor VPR presents a more convenient and cost-effective alternative compared to traditional indoor localization methods that rely on WiFi or Radio Frequency Identification (RFID) [8]. This highlights the importance of further research and innovation to develop robust and efficient VPR techniques tailored specifically for indoor environments. We argue that the suboptimal performance of current VPR methods in indoor environments can be primarily attributed to the repeated structure caused by the repetitive and symmetrical designs of man-made buildings. Unlike outdoor environments, indoor spaces often exhibit high visual similarity across different locations (see Fig. 1), particularly in multi-floor buildings where architectural designs, floor layouts, and decorative elements are often highly repetitive [9]–[11]. Geometry-based verification approaches are susceptible to false positive correspondences in environments with repetitive structures [12], which significantly undermines the reliability of place recognition in unmanned systems.

Inspired by human cognitive patterns, several recent studies [13]–[17] proposed leveraging the high-level semantic information embedded in scene texts for robot localization. However, these methods also typically rely on off-the-shelf Scene Text Spotting (STS) technology, which frequently becomes a computational bottleneck. Furthermore, they mainly use a predefined dictionary of specific words to filter out discriminative texts, and this limits their adaptability to

¹Southern University of Science and Technology, Shenzhen, China. taohq2024@mail.sustech.edu.cn.

²Peng Cheng Laboratory, Shenzhen, China.

³University of Cambridge, Cambridge, United Kingdom.

*Corresponding authors: Bingxi Liu liubx@pcl.ac.cn and Hong Zhang hzhang@sustech.edu.cn.

This work was supported in part by the Shenzhen Science and Technology Program (No. SGDX20240115111759002), in part by the Meituan Academy of Robotics Shenzhen, and in part by the SUSTech High-Level Special Funds (No. G03034K003).

diverse environments and requires significant manual effort. Additionally, existing text-based localization datasets, which are collected with a focus on scene texts, remain limited in number. Most of these datasets deliberately capture scene texts from close distances and frontal viewpoints to facilitate text spotting. However, such data collection strategies do not accurately reflect the typical visual conditions encountered in robot navigation within real-world environments.

To enhance the applicability of VPR in indoor settings, we propose **TextInPlace**, a unique dual-branch VPR framework that harnesses textual clues for robust spatial verification in highly repetitive indoor environments. Specifically, TextInPlace performs coarse-grained retrieval based on the global descriptor derived from the VPR branch, and executes scene text spotting via a dedicated STS branch applied to both query and retrieved images. Discriminative texts are efficiently filtered out based on predefined rules or, more generally, using a large language model (LLM). It then establishes textual semantic correspondence by matching these discriminative scene texts, enabling explainable re-ranking of the top-K candidate images initially retrieved by VPR branch. Moreover, the VPR branch and STS branch are combined with a local parameter sharing backbone for optimizing computational efficiency. To address the limitations of existing datasets, we use a panoramic camera to establish an indoor VPR benchmark dataset, called **Maze-with-Text**. The panoramic images are then cropped to generate VPR data. In addition to scene texts, most images in the dataset also capture the structural details of the surrounding environment.

Our main contributions can be summarized as follows:

- We propose TextInPlace, a unique VPR framework that generates global descriptors and performs scene text spotting through a unified local parameter sharing network, which can optimize computational efficiency.
- We develop an LLM-based text filter that flexibly and generically identifies discriminative texts.
- We establish Maze-with-Text, an indoor VPR benchmark dataset to highlight the challenge of repetitive structures in multi-floor buildings, with scene texts appearing at various distances and perspectives, thus more closely reflecting robot navigation scenarios.
- We achieve SOTA results on both custom and public datasets, demonstrating the robustness of text-based spatial verification in repetitive indoor environments.

II. RELATED WORK

A. Visual Place Recognition Network

The VPR network consists mainly of backbone architecture and aggregation layer. Both CNN-based [3] [4] [18] and Transformer-based [19] [20] feature extraction backbones have been widely employed in VPR research, demonstrating their effectiveness. Recently, researchers adopted the vision foundation model DINOv2 [21] as a backbone, exploring both train-free [22] and fine-tuning [23] [24] approaches, and achieving remarkable capabilities. However, vision foundation models are computationally intensive, and relying on

large backbones may lead researchers to overlook innovations in other aspects of the VPR problem [25]. The role of the aggregation layer is to compress high-dimensional feature maps into a feature vector, serving as a global descriptor. Early aggregation layers, including NetVLAD [26], GeM [27] and ConvAP [28], are primarily designed to be integrated with CNN-based backbone networks for enhanced feature representation. With the exceptional performance exhibited by the DINOv2, researchers also introduced novel aggregation techniques, such as SALAD [29], specifically designed for networks utilizing DINOv2 as their backbone. More recently, BoQ [30] introduced an attention-based aggregation method, which leverages learned queries to enhance feature aggregation. However, most current VPR research primarily focuses on outdoor scenarios. Recent studies, such as AnyLoc [22] and VLAD-BuFF [25], highlighted the poor generalization of outdoor-trained models to indoor and structured environments.

Datasets are another crucial component of learning-based VPR methods. Unlike outdoor VPR datasets, indoor VPR datasets are difficult to obtain from online resources and often require self-collection, resulting in relatively smaller scales. NYC-Indoor-VPR [31] introduced an indoor VPR dataset with a semi-automatic annotation method to mitigate the data scarcity in indoor VPR research. Additionally, existing large-scale indoor visual localization datasets, such as RISEdb [32] and Naver Labs [33], can also generate VPR labels by processing the 6-degree-of-freedom (6-DOF) poses associated with the images.

B. Text-based Localization and Place Recognition

In recent years, text-based localization methods have emerged as a promising solution for achieving robust localization in challenging environments. The high-level semantic features of scene texts demonstrate remarkable invariance to illumination changes and viewpoint variations. Moreover, these features offer effective discriminative capabilities in highly repetitive scenes. TextPlace [14] is the first to utilize scene texts for VPR in the context of topological localization. It demonstrates that scene text can effectively mitigate the challenges posed by extreme visual appearance variations in urban environments. TextSLAM [15] is the first work that tightly integrates texts semantic information for loop closure detection (LCD) in visual SLAM. Recently, TextLCD [17] integrated a multi-modal LCD method based on explicit scene texts into LiDAR SLAM frameworks and introduced a text-based repetitive scene dataset. However, these methods have two main limitations: (1) They treat scene text spotting as an independent module, leading to a decrease in system computational efficiency, and (2) most of these methods rely on a predefined dictionary to filter key texts, which significantly limits their adaptability to different environments. Furthermore, most existing methods depend on spatial-temporal constraints to construct text maps, whereas the VPR problem typically operates without temporal constraints.

III. METHODOLOGY

In this section, we provide a detailed discussion of our proposed TextInPlace framework, including its core components

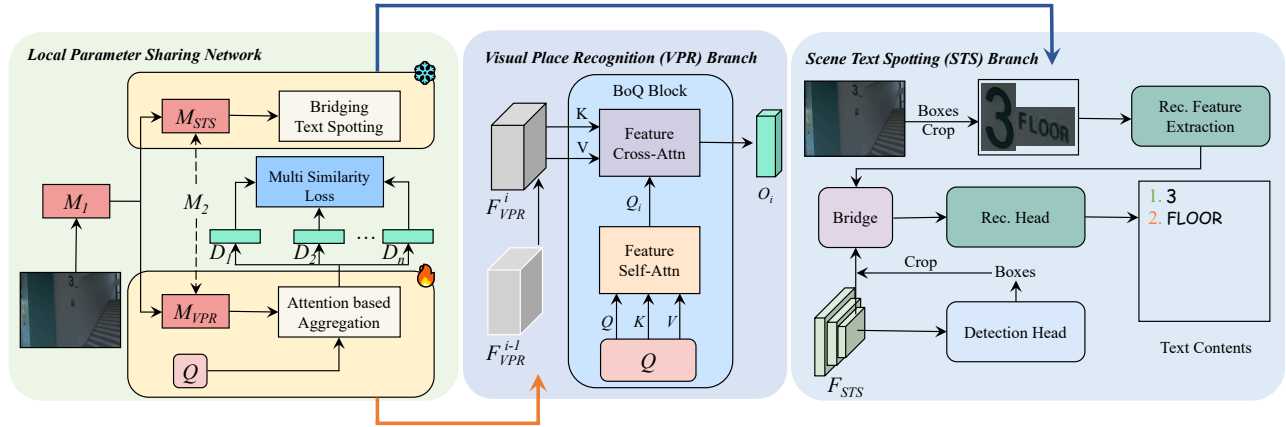


Fig. 2. An overview of TextInPlace framework. TextInPlace is (a) a local parameter sharing network with two branches. (b) The Visual Place Recognition Branch extracts global descriptors for coarse global retrieval. (c) The Scene Text Spotting Branch detects and recognizes scene texts in query and database images. Finally, re-ranking is performed based on the text similarity between the query image and the retrieved images.

and training methodology. The model architecture features a dual-branch design within a local parameter sharing network, as depicted in Fig. 2.

A. The Local Parameter Sharing Network for Multi-task

The input images I are processed by a pre-trained model M to obtain feature maps F with dimensions $C \times H \times W$. The pre-trained model can be a classic model such as ResNet [34], a more recent model like DINOv2 [21], or other future models. We decompose M into two components: M_1 and M_2 . To ensure efficient inference and smooth multi-task performance, the parameters of M_1 are frozen during training. In contrast, M_2 is shared and reused across both the visual place recognition branch, denoted as M_{VPR} , and the scene text spotting branch, denoted as M_{STS} .

B. The Visual Place Recognition Branch

Effective aggregation of multi-channel feature maps is crucial for accurate and fast VPR. To address this, we remove the fully connected layer in M_{VPR} and attach an aggregator M_{agg} based on Multi-Head Attention (MHA). This mechanism, defined as:

$$\text{MHA}(q, k, v) = \text{softmax}\left(\frac{q \cdot k^\top}{\sqrt{d}}\right)v, \quad (1)$$

plays a key role in dynamically assessing the relevance of input features.

Specifically, we follow the aggregation block described in Bag-of-Queries (BoQ) [30] and introduce a set of learnable queries that interact with the multi-channel feature maps F_{VPR} through cross-attention. Each block contains a fixed set of learnable queries, denoted as Q . The process begins by applying self-attention to Q :

$$Q_i = \text{MHA}(Q, Q, Q) + Q, \quad (2)$$

where i represents the block index. This step enables the learnable queries to integrate shared contextual information during the training phase.

Next, the output Q_i is passed along with the feature maps F_{VPR}^i to a cross-attention layer:

$$O_i = \text{MHA}(Q_i, F_{VPR}^i, F_{VPR}^i), \quad (3)$$

where F_{VPR}^i denotes the feature maps input to the i -th cross-attention layer. These feature maps are generated by passing F_{VPR}^{i-1} through a transformer-encoder. The outputs from all blocks are then concatenated:

$$O = \text{Concat}(O_1, O_2, \dots, O_i), \quad (4)$$

and passed through a linear projection layer to reduce the dimensionality of the final descriptor.

These learnable queries are trainable parameters independent of the input features and dynamically aggregate information by computing attention weights between the query and feature maps.

C. The Scene Text Spotting Branch

To enable robust and efficient scene text spotting, we adopt a well-trained detector M_{det} and recognizer M_{rec} . These modules are developed and trained independently, allowing flexible replacement and updates as needed. To further enhance their accuracy and synergy, we use an adapter M_{ada} and bridge M_{bri} proposed in [35] to facilitate improved coordination between these modules.

Given a feature map F_{STS} , the detection process proceeds as follows:

$$P_{det} = M_{det}(F_{STS}), \quad (5)$$

where P_{det} represents the predictions of the detector. After obtaining these predictions, we extract the corresponding regions from both the original input image I and the feature map F_{STS} generated by the detection backbone. This extraction process is defined as:

$$F_{crop} = \text{Crop}(F_{STS}, P_{det}), \quad I_{crop} = \text{Crop}(I, P_{det}), \quad (6)$$

where Crop denotes the crop operation based on the detector's output.

The cropped regions are then passed to the recognizer:

$$F_{\text{rec}} = M_{\text{rec}}(I_{\text{crop}}), \quad (7)$$

where F_{rec} represents the recognition features generated by the recognition backbone. Finally, both the recognition features F_{rec} and the cropped features from the detection backbone F_{crop} are sent to the bridge module for further processing, ensuring enhanced feature integration and consistency.

The bridge module, M_{bri} , is composed of a convolutional layer, a MHA layer, and a linear layer. The operation is defined as:

$$F = F_{\text{rec}} + \text{Linear}(\text{MHA}(\text{Conv}(F_{\text{crop}}))), \quad (8)$$

where this module addresses the challenges of error accumulation and sub-optimal performance typically encountered in two-step spotting pipelines, while preserving modularity.

The adapter module, M_{ada} , comprises two linear layers and an activation function. It is inserted between the detector M_{det} and the recognizer M_{rec} to enhance the synergy between these components by refining the intermediate features and improving feature alignment between the two stages.

D. Verification based on Discriminative Scene Text

Once the query descriptor O is extracted, a K-nearest neighbor (KNN) search is performed in the existing feature database D based on Euclidean distance. The top-K results are selected. Subsequently, the scene texts T extracted from the query image is compared with the texts from the top-K results. It is important to note that certain text elements in scenes, such as "Fire Hydrant" or "Emergency Exit", may appear frequently across various locations, leading to potential perceptual ambiguity. To address this issue, we propose two solutions.

1) *Rule-based Text Filter*: In indoor environments, numerical identifiers, such as door numbers, are commonly used to distinguish repetitive structures. Consequently, our rule-based text filter identifies and filters discriminative texts by detecting the presence of numerical digits within the texts.

2) *LLM-based Text Filter*: Due to the vast commonsense knowledge of the LLM, it can handle complex scene texts more flexibly. As shown in Fig. 3, when provided with a prompt, the LLM can automatically discern discriminative texts. Specifically, our implementation utilizes the GPT-4o-mini API for LLM-based text filter.

Text is extracted from a scene image for place recognition, such as door numbers. Please note that some texts do not have the localization capabilities and may not be distinctive, such as "Fire Hydrant" "12345" or "Emergency Exit". If the numbers in the text imply floor information, please make sure they belong to the same floor. Your task is to filter the discriminative and meaningful text within the query text and respond following the example format.

Query text: "4F 401 Hydrant FUNE Fire K 12345 12561112 1 4". Answer the distinctive texts only. (If there is no distinctive texts, please reply None.)
Your output: 4F, 401, 4

Query text: "501 Mitte MANHALKUN BONNES Fire Hydrant Exit 5F". Answer the distinctive texts only.

501, 5F

Fig. 3. An example prompt for the LLM-based text filter.

When discriminative texts are filtered, the re-ranking and verification are conducted using a string similarity score, defined as follows:

$$\text{Score}_{\text{sim}}(T_{\text{query}}, T_{\text{db}}) = \frac{|T_{\text{query}} \cap T_{\text{db}}|}{|T_{\text{query}}|}, \quad (9)$$

where T_{query} and T_{db} are the sets of detected text strings in the query image and database image, respectively. The intersection denotes matching text segments, and the score ranges between 0 and 1. The results are re-ranked based on this score, with higher scores indicating better matches.

E. Training Process

In the TextInPlace framework, only the VPR branch composed of M_{VPR} and M_{agg} requires training. We adopt a two-phase training strategy for the VPR branch, beginning with training on a large-scale outdoor dataset and subsequently fine-tuning it using indoor data.

1) *Indoor VPR Dataset for Fine-tuning*: Due to the limited availability of high-quality indoor VPR training datasets, we propose converting 6-DOF ground truth data from visual localization datasets into VPR labels. This approach enables the fine-tuning of outdoor-trained VPR models for indoor domains, effectively bridging the data gap and improving model performance. Following Berton et al. [3], we split the position coordinates $\{x, y\}$ into square geographical cells, and further slice each cell into a set of classes according to the direction/heading $\{\text{heading}\}$ of each image. Formally, the image set assigned to the class F_{e_i, n_j, h_k} would be

$$\left\{ f : \left\lfloor \frac{x}{M} \right\rfloor = e_i, \left\lfloor \frac{y}{M} \right\rfloor = n_j, \left\lfloor \frac{\text{heading}}{\alpha} \right\rfloor = h_k \right\}, \quad (10)$$

where M and α are two parameters that define the spatial and angular boundaries of each class.

2) *Loss function*: We use the multi-similarity loss [36] to train the VPR branch. For i -th image in training dataset, D_i is the corresponding global descriptors, and \mathcal{P}_i and \mathcal{N}_i represent the sets of positive pairs and negative pairs, respectively. s_{ij} is the cosine similarity between global descriptors of D_i and D_j . The loss for samples can be computed as follows:

$$\mathcal{L}_{\text{MS}} = \frac{1}{N} \sum_{i=1}^N \left\{ \frac{1}{\alpha} \log \left[1 + \sum_{j \in \mathcal{P}_i} e^{-\alpha(s_{ij} - \lambda)} \right] + \frac{1}{\beta} \log \left[1 + \sum_{j \in \mathcal{N}_i} e^{\beta(s_{ij} - \lambda)} \right] \right\}, \quad (11)$$

where α , β , and λ are hyperparameters that regulate the weighting of the positive and negative components.

IV. THE MAZE-WITH-TEXT DATASET

To the best of our knowledge, TextLCD [17] is the most suitable publicly available dataset for evaluating our framework, as it features repetitive structures and scene texts. However, the scale of the TextLCD dataset is limited, as it was collected from only three floors. Thus, it fails to capture the perceptual confusion caused by repetitive structures across multiple floors. Moreover, to simplify text spotting, a

significant portion of the text images were captured at close distances and frontal viewpoints, which does not reflect the environmental structure. This also does not align with the typical scenarios encountered during robot navigation.

To address these limitations and inspired by the semi-automatic annotation method of NYC-Indoor-VPR [31], we develop the Maze-with-Text dataset within a university teaching building. First, we use a handheld Insta360 One X3 spherical camera to record videos at 3840×1920 resolution across five floors. The higher resolution, relative to that of NYC-Indoor-VPR (1920×960), facilitates clearer capture of scene texts for improved detection and recognition. On each floor, two videos are captured along approximately the same trajectory at different times, serving as the query and database sets, respectively. These panoramic videos are then processed using OpenVSLAM [37] to generate a set of keyframes and topological trajectories. Finally, the turning points of the topological trajectories are manually matched to align the keyframe poses within the same coordinate frame. To avoid false positive loop closure detection, it is manually enabled only when the trajectory exhibits clear intersections.

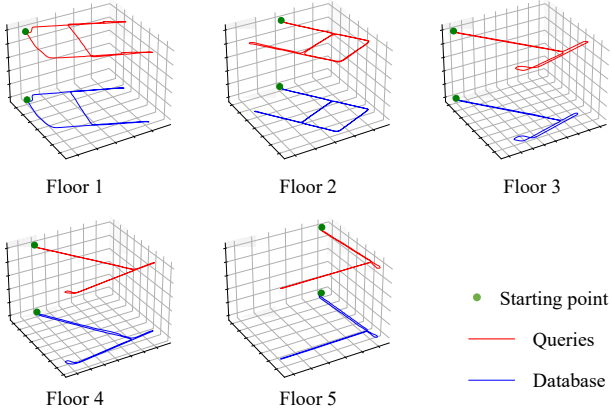


Fig. 4. Illustrations of the trajectories in our dataset.

The trajectories of the dataset sequences are illustrated in Fig. 4. Keyframes are used as the images in the dataset. Each equirectangular projection image is cropped into four perspective images with a resolution of 640×480 and a 90° field of view (FOV). In addition, a text detector is employed to identify and retain images containing scene texts, which are then used as query images. Table I provides the number of images in the Maze-with-Text dataset.

TABLE I

NUMBER OF IMAGES IN THE MAZE-WITH-TEXT DATASET

	Floor 1	Floor 2	Floor 3	Floor 4	Floor 5	All
Queries	280	253	258	245	269	1305
Database	1368	2268	1588	1720	1596	8540

V. EXPERIMENTS

This section reports detailed experimental settings and evaluation results on two indoor test datasets with repetitive structures, namely Maze-with-Text and TextLCD dataset.

A. Implementation details

The proposed method is implemented using PyTorch [38] with model training conducted on two NVIDIA RTX 3090

GPUs, while testing is performed on a single GPU. We employ ResNet-50 [34] backbone for feature extraction. DPTText-DETR [39] is employed for text detection, while DiG [40] is adopted for text recognition. Our method defaults to using a rule-based text filter, while the variant utilizing a LLM-based text filter is designated as TextInPlace-L.

We initially train the model on the GSV-Cites dataset [28], a large-scale urban dataset that includes 524k images and spans 62k distinct locations. To enable the model to generalize to indoor environments, it is fine-tuned using our reorganized Naver Labs dataset [33], as detailed in Section III-E.1. Regarding hyperparameters, M is set to 2, and α is set to 3. During the training phases, we use the AdamW optimizer with the learning rate set to 1×10^{-4} for initial training and 5×10^{-5} for fine-tuning. The batch size set to 64 places, each represented by 4 images. Moreover, training process runs for 10 epochs with an early stopping strategy, and all training images are resized to 320×320 .

For evaluation metrics, we utilize the evaluation metric employed in prior research [3] [18] [28] [30] [41], which entails calculating Recall@K. This metric quantifies the proportion of instances in which at least one of the top-K retrieved images falls within the predefined threshold distance of the query image. Unless otherwise specified, the test image size is set to 640×480 .

B. Comparison with State-of-the-art

Table II shows the comparison of the proposed method with previous SOTA methods, including nine 1-stage models: NetVLAD [26], SFRS [42], CosPlace [3], EigenPlaces [4], ConvAP [28], MixVPR [41], BoQ [30], SALAD [29], CricaVPR [24], and four 2-stage re-ranking models: PatchNV [43], TransVPR [19], R2Former [20], SelaVPR [23]. Since some text-based methods, like TextPlace [14], are not open-source and mostly rely on spatial-temporal constraints (e.g., odometry) to build text maps, we do not directly compare them with our method. For all comparative methods, we adopted the well-trained model provided by their official sources. Due to the constraints on input image resolution, the test image resolution for methods employing the DINOv2 as the backbone and MixVPR is set to 224×224 and 320×320 , respectively. All 2-stage methods re-rank the top-100 candidates to improve retrieval performance.

Compared to several recent SOTA approaches, our method demonstrates superior performance. TextInPlace-L exhibits a marginal performance advantage over TextInPlace, underscoring that LLM-based text filter, which dynamically adapt their filtering strategies according to the input texts, are more effective at filtering discriminative texts than static rule-based text filter. Previous VPR methods often experience significant performance degradation due to severe perceptual confusion when encountering indoor repetitive structures. Notably, methods using the visual foundation model DINOv2 as the backbone network fail to significantly outperform those based on the ResNet-50 backbone network. 2-stage methods that employ local feature-based re-ranking struggle to handle repetitive structures effectively, primarily because of the high similarity among visual elements in the scene.

TABLE II
PERFORMANCE COMPARISON ON THE MAZE-WITH-TEXT DATASET. **BEST**, **SECOND BEST**, AND **THIRD BEST** RESULTS ARE HIGHLIGHTED. WE REPORT RECALL@1 AND RECALL@5 FOR EACH METHOD.

	Method	Backbone	Dim.	Floor 1	Floor 2	Floor 3	Floor 4	Floor 5	All
1-stage	NetVLAD [26]	VGG-16	32768	82.5 / 92.9	79.8 / 92.9	64.7 / 84.5	76.7 / 93.9	63.6 / 86.6	58.2 / 76.7
	SFRS [42]	VGG-16	4096	86.1 / 96.4	89.7 / 98.4	71.7 / 91.5	84.9 / 95.1	56.5 / 80.7	59.5 / 77.5
	CosPlace [3]	ResNet-50	2048	85.0 / 97.1	82.6 / 93.3	53.5 / 74.0	81.2 / 95.9	37.6 / 52.8	50.0 / 65.6
	EigenPlaces [4]	ResNet-50	2048	88.6 / 96.8	90.1 / 98.0	71.7 / 91.9	85.3 / 97.1	56.1 / 81.0	60.9 / 77.5
	ConvAP [28]	ResNet-50	4096	85.7 / 98.2	85.0 / 94.9	63.6 / 82.6	88.6 / 94.7	48.0 / 68.4	62.8 / 78.9
	MixVPR [41]	ResNet-50	4096	89.3 / 97.9	85.8 / 98.0	64.3 / 83.3	86.9 / 98.0	45.0 / 63.6	62.4 / 79.3
	BoQ [30]	ResNet-50	16384	87.5 / 95.7	85.4 / 95.7	77.1 / 92.3	87.7 / 97.1	66.2 / 89.2	67.5 / 84.1
	DINOv2-BoQ [30]	DINOv2-B	12288	89.3 / 96.8	88.5 / 98.0	74.0 / 89.5	89.0 / 98.4	59.5 / 79.6	65.7 / 80.8
2-stage	SALAD [29]	DINOv2-B	8448	87.5 / 95.4	83.4 / 94.9	67.8 / 86.8	88.6 / 98.8	47.6 / 68.8	61.6 / 75.6
	CricaVPR [24]	DINOv2-B	4096	86.1 / 97.5	84.2 / 94.5	66.3 / 84.5	85.3 / 96.7	47.6 / 68.4	57.7 / 75.9
	Patch-NV [43]	VGG-16	2826 × 4096	90.7 / 95.0	90.5 / 96.8	76.4 / 90.3	84.9 / 95.5	62.8 / 83.3	65.0 / 77.5
	TransVPR [19]	ViT	1200 × 256	85.4 / 95.0	85.8 / 94.9	77.1 / 91.5	82.4 / 92.4	69.1 / 90.7	62.9 / 78.4
2-stage	R2Former [20]	ViT	500 × 131	73.3 / 93.9	83.8 / 96.0	64.3 / 82.9	68.6 / 88.2	52.8 / 81.8	61.1 / 75.6
	SelaVPR [23]	DINOv2-L	61 × 61 × 128	85.4 / 95.4	76.3 / 88.5	75.6 / 90.3	79.6 / 93.1	62.1 / 78.8	56.7 / 71.9
	TextInPlace	ResNet-50	16384	92.9 / 96.8	97.2 / 100.0	85.3 / 95.3	89.0 / 94.7	83.6 / 96.7	85.4 / 93.9
	TextInPlace-L	ResNet-50	16384	92.9 / 97.1	96.4 / 99.6	86.0 / 96.1	89.0 / 97.6	84.0 / 98.5	86.1 / 95.5

Our method addresses this challenge by leveraging scene texts as positional clues, enabling robots to distinguish such scenes in a human-like manner.

To further validate our experimental findings, we conduct comparative evaluations on a public dataset. Specifically, we selected sequences seq1, seq2, and seq4 from the TextLCD dataset [17]. The initial segments of each trajectory serves as the database, while the overlapping subsequent trajectory served as queries. To more closely align with the application of loop closure detection, we select one query image every 3 seconds. It means that scene texts may not always be present in the query images.

As shown in Table III, our method achieves the significant improvement on seq2, surpassing BoQ by 5.7% in Recall@1. On seq1 and seq4, it maintains performance comparable to that of BoQ. Both the 2-stage method, Patch-NV, and the DINOv2-based method, SALAD, demonstrate inferior performance compared to TextInPlace.

TABLE III

PERFORMANCE COMPARISON ON TEXTLCD TEST DATASET. THE BEST IS HIGHLIGHTED IN **BOLD** AND THE SECOND-BEST IS UNDERLINED.

Method	Backbone	Indoor corridor (seq1)		Indoor corridor (seq2)		Semi-indoor corridor (seq4)	
		R@1	R@5	R@1	R@5	R@1	R@5
Patch-NV [43]	VGG-16	75.7	<u>87.6</u>	69.6	83.7	93.0	<u>93.0</u>
SALAD [29]	DINOv2-B	80.4	<u>85.0</u>	56.0	66.7	<u>84.5</u>	90.1
BoQ [30]	ResNet-50	84.1	88.8	<u>71.6</u>	77.3	93.0	94.0
TextInPlace	ResNet-50	<u>83.2</u>	88.8	<u>77.3</u>	<u>81.6</u>	93.0	<u>93.0</u>

Since TextLCD is a multi-modal LiDAR-based LCD method, a direct comparison with our visual approach is not feasible. However, the original TextLCD paper [17] shows that its recall is lower than SALAD, which we attribute to its reliance on text-derived semantic and geometric information,

neglecting appearance information. In contrast, our method incorporates global descriptors as prior information and uses discriminative texts for spatial verification, outperforming SALAD. Therefore, we argue TextInPlace theoretically outperforms TextLCD in repetitive indoor environments.

C. Ablation Study

1) *Selection of Fine-tuning Dataset*: In Table IV, we select three indoor datasets, namely NYC-Indoor [31], RISEdb [32], and Naver Labs [33], for fine-tuning experiments. Among them, models fine-tuned on NYC-Indoor and RISEdb exhibit a decline in performance compared to their pre-fine-tuned states. In contrast, fine-tuning with Naver Labs leads to significant performance improvements, especially on the floor 5 subdataset.

TABLE IV
ABLATION STUDY ON FINE-TUNING WITH DIFFERENT TRAINING SET.

ID	Indoor dataset			R@1	
	NYC-Indoor	RISEdb	Naver labs	Floor 5	All
1				59.5	67.7
2	✓			46.1	59.6
3			✓	55.8	56.0
4				✓	72.9 72.5

2) *Effectiveness of Re-ranking and Fine-tuning*: As shown in Table V, We conduct ablation studies to evaluate the impact of re-ranking and fine-tuning in our method. Experimental results indicate that under a repetitive structure, text-based re-ranking effectively mitigates perceptual confusion caused by similar appearances. Indoor domain fine-tuning enhances the ability of our model to learn structured features specific to indoor environments. Notably, the combination of these two components leverages their individual strengths, resulting in robust and improved performance.

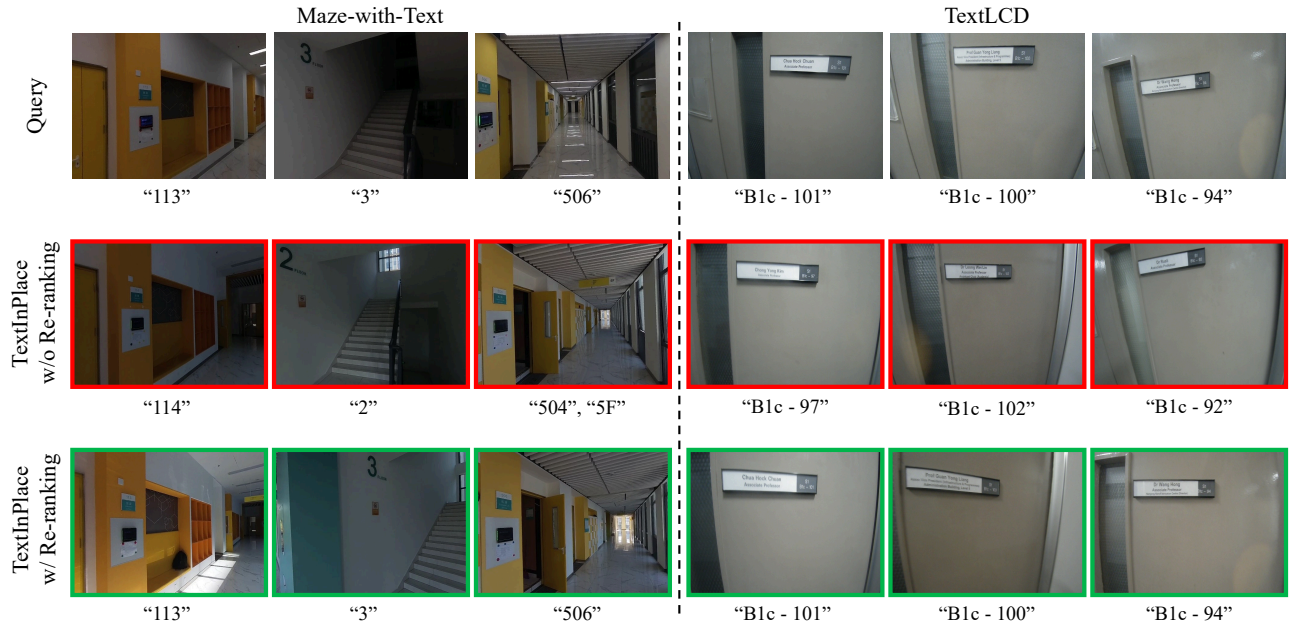


Fig. 5. Examples of retrieval results for challenging queries. Each column corresponds to one query case. The first three columns are from the Maze-with-Text dataset, and the last three columns are from the TextLCD dataset. The first row displays the query image, while the other two rows show the top-1 retrieved images. Incorrect retrievals are distinguished by a red border, whereas correct retrievals are highlighted with a green border. Below each image is the discriminative scene text extracted from the image.

TABLE V
ABLATION STUDY ON RE-RANKING AND FINE-TUNING.

ID	Re-rank	Fine-tune	Floor 5		All	
			R@1	R@5	R@1	R@5
1			59.5	80.7	67.7	83.8
2	✓		78.4 +18.9	90.7 +10.0	81.4 +13.7	91.4 +7.6
3		✓	72.9 +13.4	93.7 +13.0	72.5 +4.8	89.4 +5.6
4	✓	✓	83.6 +24.1	96.7 +16.0	85.4 +17.7	93.9 +10.1

D. Complexity Analysis

The complexity of the network plays a vital role in practical applications. In Table VI, we compare the computational cost of our proposed method with the baseline method (BoQ + DG-Bridge Spotter) on our all floors dataset. In contrast to our approach, the baseline method employs BoQ [30] for image retrieval and DG-Bridge Spotter [35] for text-based re-ranking as separate processes. Our method achieves notable efficiency improvements, particularly in extraction time and STS time. These results underscore the effectiveness of our local parameter sharing network in minimizing computational latency. In the future, we can replace the text detection and recognition modules with more lightweight alternatives to further reduce the time consumption of STS. Additionally, TextInPlace-L incurs significantly higher time consumption during the re-ranking stage compared to TextInPlace, primarily due to its reliance on remote LLM access.

E. Visualization

Fig. 5 shows detailed cases where repetitive structures cause significant perceptual confusion. When relying solely on visual descriptors, global retrieval fails in the top-1 results. However, by applying text-based verification, our method successfully finds the correct reference image. This

TABLE VI
COMPARISON OF COMPUTATIONAL COST.

Method	Latency per Query (ms)			
	Extrac.	Retrival	STS	Re-rank
BoQ + DG-Bridge Spotter	7.7	2.9	165.7	0.1
TextInPlace	5.9	2.9	161.0	0.1
TextInPlace-L	5.9	2.9	161.0	962.8

demonstrates the effectiveness of our approach in using text-based verification to alleviate the perceptual confusion caused by repetitive structures. Furthermore, our dataset not only includes scene texts but also captures the environmental structure, making it a more accurate reflection of real-world robot navigation scenarios compared to TextLCD.

VI. CONCLUSIONS

To address the challenge of VPR in repetitive indoor environments, TextInPlace is proposed to enable coarse-grained image retrieval using global descriptors, followed by spatial verification through discriminative scene texts. Extensive experiments conducted on the newly proposed Maze-with-Text dataset, as well as the publicly available TextLCD dataset, demonstrate that the proposed TextInPlace can achieve state-of-the-art performance against perceptual aliasing caused by repetitive indoor structures. Our code and dataset are available for the benefit of the community.

ACKNOWLEDGMENT

The authors would like to thank Tongxing Jin, Thien-Minh Nguyen, Xinhang Xu, Yizhuo Yang, Shenghai Yuan, Jianping Li and Lihua Xie for the contribution of the TextLCD dataset [17] and for allowing its academic use.

REFERENCES

[1] S. Lowry, N. Sünderhauf, P. Newman, J. J. Leonard, D. Cox, P. Corke, and M. J. Milford, “Visual place recognition: A survey,” *IEEE Trans. Robot.*, vol. 32, no. 1, pp. 1–19, 2015.

[2] S. Schubert, P. Neubert, S. Garg, M. Milford, and T. Fischer, “Visual place recognition: A tutorial,” *IEEE Robot. Autom. Mag.*, vol. 31, no. 3, pp. 139–153, 2023.

[3] G. Berton, C. Masone, and B. Caputo, “Rethinking visual geo-localization for large-scale applications,” in *Proc. IEEE/CVF Conf. Comput. Vis. Pattern Recognit.*, 2022, pp. 4878–4888.

[4] G. Berton, G. Trivigno, B. Caputo, and C. Masone, “Eigenplaces: Training viewpoint robust models for visual place recognition,” in *Proc. Int. Conf. Comput. Vis.*, 2023, pp. 11 080–11 090.

[5] B. Liu, Y. Fu, F. Lu, J. Cui, Y. Wu, and H. Zhang, “Npr: Nocturnal place recognition using nighttime translation in large-scale training procedures,” *IEEE J. Sel. Top. Signal Process.*, 2024.

[6] M. J. Milford and G. F. Wyeth, “Seqslam: Visual route-based navigation for sunny summer days and stormy winter nights,” in *Proc. IEEE Int. Conf. Robot. Autom.*, 2012, pp. 1643–1649.

[7] O. Grainge, M. Milford, I. Bodala, S. D. Ramchurn, and S. Ehsan, “Design space exploration of low-bit quantized neural networks for visual place recognition,” *IEEE Robot. Autom. Lett.*, 2024.

[8] Z. Guo and Y. Zhu, “Visual place recognition datasets for indoor spaces,” in *Proc. IEEE Int. Conf. Multimedia and Expo*, 2023, pp. 1571–1576.

[9] A. Jaenal, F.-A. Moreno, and J. Gonzalez-Jimenez, “Unsupervised appearance map abstraction for indoor visual place recognition with mobile robots,” *IEEE Robot. Autom. Lett.*, vol. 7, no. 3, pp. 8495–8501, 2022.

[10] P. Kaveti, A. Gupta, D. Giaya, M. Karp, C. Keil, J. Nir, Z. Zhang, and H. Singh, “Challenges of indoor slam: A multi-modal multi-floor dataset for slam evaluation,” in *Proc. IEEE Int. Conf. Autom. Sci. Eng.*, 2023, pp. 1–8.

[11] H. Taira, M. Okutomi, T. Sattler, M. Cimpoi, M. Pollefeys, J. Sivic, T. Pajdla, and A. Torii, “Inloc: Indoor visual localization with dense matching and view synthesis,” in *Proc. IEEE/CVF Conf. Comput. Vis. Pattern Recognit.*, 2018, pp. 7199–7209.

[12] J. Yu, H. Ye, J. Jiao, P. Tan, and H. Zhang, “Gv-bench: Benchmarking local feature matching for geometric verification of long-term loop closure detection,” in *Proc. IEEE/RSJ Int. Conf. Intell. Robots Syst.*, 2024, pp. 7922–7928.

[13] H.-C. Wang, C. Finn, L. Paull, M. Kaess, R. Rosenholtz, S. Teller, and J. Leonard, “Bridging text spotting and slam with junction features,” in *Proc. IEEE/RSJ Int. Conf. Intell. Robots Syst.*, 2015, pp. 3701–3708.

[14] Z. Hong, Y. Petillot, D. Lane, Y. Miao, and S. Wang, “Textplace: Visual place recognition and topological localization through reading scene texts,” in *Proc. Int. Conf. Comput. Vis.*, 2019, pp. 2861–2870.

[15] B. Li, D. Zou, Y. Huang, X. Niu, L. Pei, and W. Yu, “Textslam: Visual slam with semantic planar text features,” *IEEE Trans. Pattern Anal. Mach. Intell.*, 2023.

[16] H. Li, S. Yu, S. Zhang, and G. Tan, “Resolving loop closure confusion in repetitive environments for visual slam through ai foundation models assistance,” in *Proc. IEEE Int. Conf. Robot. Autom.*, 2024, pp. 6657–6663.

[17] T. Jin, T.-M. Nguyen, X. Xu, Y. Yang, S. Yuan, J. Li, and L. Xie, “Robust loop closure by textual cues in challenging environments,” *IEEE Robot. Autom. Lett.*, 2024.

[18] G. Berton, R. Mereu, G. Trivigno, C. Masone, G. Csurka, T. Sattler, and B. Caputo, “Deep visual geo-localization benchmark,” in *Proc. IEEE/CVF Conf. Comput. Vis. Pattern Recognit.*, 2022, pp. 5396–5407.

[19] R. Wang, Y. Shen, W. Zuo, S. Zhou, and N. Zheng, “Transvpr: Transformer-based place recognition with multi-level attention aggregation,” in *Proc. IEEE/CVF Conf. Comput. Vis. Pattern Recognit.*, 2022, pp. 13 648–13 657.

[20] S. Zhu, L. Yang, C. Chen, M. Shah, X. Shen, and H. Wang, “R2former: Unified retrieval and reranking transformer for place recognition,” in *Proc. IEEE/CVF Conf. Comput. Vis. Pattern Recognit.*, 2023, pp. 19 370–19 380.

[21] M. Oquab, T. Dariseti, T. Moutakanni, H. Vo, M. Szafraniec, V. Khalidov, P. Fernandez, D. Haziza, F. Massa, A. El-Nouby *et al.*, “Dinov2: Learning robust visual features without supervision,” *Trans. Mach. Learn. Res.*, pp. 1–31, 2024.

[22] N. Keetha, A. Mishra, J. Karhade, K. M. Jatavallabhula, S. Scherer, M. Krishna, and S. Garg, “Anyloc: Towards universal visual place recognition,” *IEEE Robot. Autom. Lett.*, 2023.

[23] F. Lu, L. Zhang, X. Lan, S. Dong, Y. Wang, and C. Yuan, “Towards seamless adaptation of pre-trained models for visual place recognition,” in *Proc. 12th Int. Conf. Learn. Representations*, 2024.

[24] F. Lu, X. Lan, L. Zhang, D. Jiang, Y. Wang, and C. Yuan, “Cricavpr: Cross-image correlation-aware representation learning for visual place recognition,” in *Proc. IEEE/CVF Conf. Comput. Vis. Pattern Recognit.*, 2024, pp. 16 772–16 782.

[25] A. Khalil, M. Xu, S. Hausler, M. Milford, and S. Garg, “Vlad-buff: Burst-aware fast feature aggregation for visual place recognition,” in *Proc. Eur. Conf. Comput. Vis.*, 2025, pp. 447–466.

[26] R. Arandjelovic, P. Gronat, A. Torii, T. Pajdla, and J. Sivic, “Netvlad: Cnn architecture for weakly supervised place recognition,” in *Proc. IEEE/CVF Conf. Comput. Vis. Pattern Recognit.*, 2016, pp. 5297–5307.

[27] F. Radenović, G. Tolias, and O. Chum, “Fine-tuning cnn image retrieval with no human annotation,” *IEEE Trans. Pattern Anal. Mach. Intell.*, vol. 41, no. 7, pp. 1655–1668, 2018.

[28] A. Ali-bey, B. Chaib-draa, and P. Giguere, “Gsv-cities: Toward appropriate supervised visual place recognition,” *Neurocomputing*, vol. 513, pp. 194–203, 2022.

[29] S. Izquierdo and J. Civera, “Optimal transport aggregation for visual place recognition,” in *Proc. IEEE/CVF Conf. Comput. Vis. Pattern Recognit.*, 2024, pp. 17 658–17 668.

[30] A. Ali-bey, B. Chaib-draa, and P. Giguere, “Boq: A place is worth a bag of learnable queries,” in *Proc. IEEE/CVF Conf. Comput. Vis. Pattern Recognit.*, 2024, pp. 17 794–17 803.

[31] D. Sheng, A. Yang, J.-R. Rizzo, and C. Feng, “Nyc-indoor-vpr: A long-term indoor visual place recognition dataset with semi-automatic annotation,” in *Proc. IEEE Int. Conf. Robot. Autom.*, 2024, pp. 14 853–14 859.

[32] C. Sanchez-Belenguer, E. Wolfart, A. Casado-Coscolla, and V. Sequeira, “Risedb: a novel indoor localization dataset,” in *Proc. IEEE Int. Conf. Pattern Recognit.*, 2021, pp. 9514–9521.

[33] D. Lee, S. Ryu, S. Yeon, Y. Lee, D. Kim, C. Han, Y. Cabon, P. Weinzaepfel, N. Guérin, G. Csurka *et al.*, “Large-scale localization datasets in crowded indoor spaces,” in *Proc. IEEE/CVF Conf. Comput. Vis. Pattern Recognit.*, 2021, pp. 3227–3236.

[34] K. He, X. Zhang, S. Ren, and J. Sun, “Deep residual learning for image recognition,” in *Proc. IEEE/CVF Conf. Comput. Vis. Pattern Recognit.*, 2016, pp. 770–778.

[35] M. Huang, H. Li, Y. Liu, X. Bai, and L. Jin, “Bridging the gap between end-to-end and two-step text spotting,” in *Proc. IEEE/CVF Conf. Comput. Vis. Pattern Recognit.*, 2024, pp. 15 608–15 618.

[36] X. Wang, X. Han, W. Huang, D. Dong, and M. R. Scott, “Multi-similarity loss with general pair weighting for deep metric learning,” in *Proc. IEEE/CVF Conf. Comput. Vis. Pattern Recognit.*, 2019, pp. 5022–5030.

[37] S. Sumikura, M. Shibuya, and K. Sakurada, “Openvslam: A versatile visual slam framework,” in *Proc. 27th ACM Int. Conf. Multimedia*, 2019, pp. 2292–2295.

[38] A. Paszke, S. Gross, F. Massa, A. Lerer, J. Bradbury, G. Chanan, T. Killeen, Z. Lin, N. Gimelshein, L. Antiga *et al.*, “Pytorch: An imperative style, high-performance deep learning library,” in *Proc. Adv. Neural Inf. Process. Syst.*, vol. 32, 2019.

[39] M. Ye, J. Zhang, S. Zhao, J. Liu, B. Du, and D. Tao, “Dptext-detr: Towards better scene text detection with dynamic points in transformer,” in *Proc. AAAI Conf. Artif. Intell.*, vol. 37, no. 3, 2023, pp. 3241–3249.

[40] M. Yang, M. Liao, P. Lu, J. Wang, S. Zhu, H. Luo, Q. Tian, and X. Bai, “Reading and writing: Discriminative and generative modeling for self-supervised text recognition,” in *Proc. 30th ACM Int. Conf. Multimedia*, 2022, pp. 4214–4223.

[41] A. Ali-Bey, B. Chaib-Draa, and P. Giguere, “Mixvpr: Feature mixing for visual place recognition,” in *Proc. IEEE/CVF Winter Conf. Appl. Comput. Vis.*, 2023, pp. 2998–3007.

[42] Y. Ge, H. Wang, F. Zhu, R. Zhao, and H. Li, “Self-supervising fine-grained region similarities for large-scale image localization,” in *Proc. Eur. Conf. Comput. Vis.*, 2020, pp. 369–386.

[43] S. Hausler, S. Garg, M. Xu, M. Milford, and T. Fischer, “Patch-netvlad: Multi-scale fusion of locally-global descriptors for place recognition,” in *Proc. IEEE/CVF Conf. Comput. Vis. Pattern Recognit.*, 2021, pp. 14 141–14 152.